Journal of Sound and Vibration 329 (2010) 1954–1967

Contents lists available at ScienceDirect

Journal of Sound and Vibration

journal homepage: www.elsevier.com/locate/jsvi

Impact-acoustics inspection of tile-wall bonding integrity via wavelet transform and hidden Markov models

B.L. Luk [a,*], K.P. Liu [a], F. Tong [b], K.F. Man [c]

[a] Department of Manufacturing Engineering and Engineering Management, City University of Hong Kong, Tat chee Avenue, Kowloon, Hong Kong
[b] Key laboratory of underwater acoustic communication and marine information technology of the minister of education, Xiamen University, Xiamen, China
[c] Department of Electronic Engineering, City University of Hong Kong, Tat chee Avenue, Kowloon, Hong Kong

ARTICLE INFO

Article history:
Received 24 December 2008
Received in revised form
26 November 2009
Accepted 27 November 2009
Handling Editor: L.G. Tham
Available online 23 December 2009

ABSTRACT

The impact-acoustics method utilizes different information contained in the acoustic signals generated by tapping a structure with a small metal object. It offers a convenient and cost-efficient way to inspect the tile-wall bonding integrity. However, the existence of the surface irregularities will cause abnormal multiple bounces in the practical inspection implementations. The spectral characteristics from those bounces can easily be confused with the signals obtained from different bonding qualities. As a result, it will deteriorate the classic feature-based classification methods based on frequency domain. Another crucial difficulty posed by the implementation is the additive noise existing in the practical environments that may also cause feature mismatch and false judgment. In order to solve this problem, the work described in this paper aims to develop a robust inspection method that applies model-based strategy, and utilizes the wavelet domain features with hidden Markov modeling. It derives a bonding integrity recognition approach with enhanced immunity to surface roughness as well as the environmental noise. With the help of the specially designed artificial sample slabs, experiments have been carried out with impact acoustic signals contaminated by real environmental noises acquired under practical inspection background. The results are compared with those using classic method to demonstrate the effectiveness of the proposed method.

1. Introduction

In metropolitan cities like Hong Kong, mosaic tile-walls are widely used on high-rise buildings for decoration and weather protection purposes. However, due to improper installation, climate corrosion or aging effects, there are increasing number of accidents related to tiles falling from heights caused by defective adhesives or poor bondings [1,2]. In view of this problem, the Hong Kong Housing, Planning and Land Bureau has finished a public consultation on mandatory building inspection in 2005. The government intends to pass a legislation to enforce the mandatory inspection for all tall buildings aged 30 years or above. As a result, there will be a great demand of effort to improve both accuracy and speed of the building inspection process. Therefore, it needs to develop an effective non-destructive testing system to facilitate quick, accurate and cost-effective inspections of high-rise building. In addition, this system can be attachable to various climbing robots [3–5] for carrying out inspection tasks on high-rise buildings. Throughout the intended inspection

* Corresponding author. Tel.: +852 2788 8673; fax: +852 2788 8423.
E-mail address: meblluk@cityu.edu.hk (B.L. Luk).

0022-460X/$ - see front matter © 2009 Elsevier Ltd. All rights reserved.
doi:10.1016/j.jsv.2009.11.038

processes, they involve no human operator working at life-threatening height. As such, the insurance premiums will be reduced significantly.

For the integrity assessments of external walls of high-rise buildings, the classic strategies such as ultrasound-echo and impact-echo extensively employed for bonding integrity inspection inside layered structures [6–9] are ruled out. It is because they need to maintain good contacts between the sensors and target specimens that is difficult or inconvenient to achieve at heights or on large testing areas. Meanwhile, other non-contact techniques such as holography, X-rays and shearography are too environment-sensitive and generally too expensive [10]. In addition, thermography is another non-contact method that can detect defects with good contrast while providing quick evaluation ability of large surfaces [11,12]. However, the traditional passive thermography method, which does not use any external heating source to generate a heat signature, can be affected easily by uneven natural heating source existed in the environment; this can make the interpretation of the results become difficult. Active thermography is a more reliable technique since a heating stimulus is applied to the targeted object in such a way that the defects on the object can be observed by thermal imaging. The technique can provide the details of the facade, such as size, depth and thermal properties of the tile defects with controlled thermal loading. However, a suitable excitation system such as array of IR lamps and high power flash lamps [11] are needed. This type of excitation systems are normally very bulky and can cause some inconvenience for operation at high rising buildings. In addition, the cost of infra-red camera is very high and generally can not be afforded by many small and medium-sized inspection companies.

The methodology of the impact acoustics strategy is based on the fact that if two bonded materials are impacted with a small and hard object, the characteristics of sounds emanated will vary depending on the bonding condition, thus offering a possible indicator of the condition without the need of fixing the sensor onto the test object. The manual operation of this method is simple, and of low cost, but it is unfortunately subjective and operator-dependent. To remove its dependence on the human determination and experience, there have been many efforts paid to automate the impact testing operation to develop a quantitative, convenient, easy-to-use and cost-effective nondestructive testing method for bonding defects characterization [13–18].

Most of the previous efforts relied on the statistical features extracted from the impact acoustic signals in frequency-domain, also known as feature-based recognition. Masanori Asano [14] derived a defect detection system based on classic spectral feature obtained from the frequency distribution impact acoustics parameters. In another frequency-distribution-based investigation [15], Huadong Wu defined the ratio of the power of the lower 1/3 frequency range to that of the overall frequency range in the impact-sound spectrum as the ''power accumulation ratio factor'', and used it to characterize the integrity of multi-layered materials. Based on the theoretical analysis of the impact dynamics, Tong developed an support vector machine (SVM) based tile-wall bonding state classifier, which employs the features extracted from the power spectrum density (PSD) as input [16].

Nonetheless, the features directly obtained from the signature spectra are found to be sensitive to the irregularities on the target surface, as the interaction between the impactor and the target surface in a nominally single tap would lead to overlapping patterns between different bonding integrities. Thus, under physical environments, where surface non-uniformity is unavoidable, the actual assessment performance of the impact-acoustic method based on the direct use of frequency-domain feature will be seriously affected. Moreover, under the adverse practical operation condition in large-scale inspection applications, hostile environmental noise will also pose serious challenges to the classic methods. When the signal is contaminated by the noise, the features associated with different bonding state may be subject to confusion and mismatch thus drastically affecting the recognition performance. These two negative factors hinder the impact acoustics based methods from converting into large-scale practical applications.

So far, there are few published investigations conducted upon the noise problem in impact acoustics method. Some works did report, and aimed to alleviate the problem caused by surface roughness, and they claimed to be good performance under the ''clean'' signals; however, it seemed not to be robust enough to noise. Tong [17] proposed a temporal feature based tile-wall bonding integrity evaluation system to overcome the confusion caused by the surface non-uniformity. It makes use of the time domain behavior of the initial acceleration impact-sound component. However, the limitation of this temporal feature based approach is that when the technique is applied to the environment contaminated by acoustic noise, the accurate extraction of the initial acceleration pattern will be seriously affected by the noise. Similarly, another related approach developed by Tong [18] adopted the spectral features processed by the principal component analysis (PCA) to deal with the impairments caused by the abnormal impact sounds. Again, the PCA result will also be distorted if the original PSD data has been contaminated by noise.

To simultaneously tackle the crucial problems caused by the physical surface roughness and the environmental noise, the proposed work incorporates a wavelet domain feature extraction method with a model-based pattern recognition technique to derive a robust solution for tile-wall bonding integrity inspection. Due to its property of self-adjusting the analysis windows according to the signal frequency, the wavelet transform has found extensive applications in the time-frequency characterization of transient signals [19,20]. In the present study, according to the time-frequency behavior of the typical impact acoustic signals, the wavelet scales where the signal component strongly reigns are selected for feature extraction. Compared to the conventional spectral method, the wavelet domain features can provide more information to facilitate the automatic recognition and mitigate the impairment of noise.

In terms of the pattern recognition method, although the aforementioned feature-based methods are effective, they are ''black box'' or ''grey box'' methods, which do not take the physical model of the system into consideration. The alternative

model-based methods, on the other hand, take the advantage of knowing the system structure and hence, are sometimes advantageous [21]. Among the model based strategies, the application of hidden Markov model (HMM) is gaining more and more attention in the fields of pattern recognition and classification associated with time series input, which is motivated by its popular success in speech recognition [22–25].

In this paper, an HMM is introduced to statistically model the temporal behavior of impact acoustic signals via the wavelet domain features to derive a robust approach for the tile-wall bonding integrity assessment at the presence of noise as well as the abnormal impacts caused by surface irregularities. To validate the effectiveness of the proposed method, numerical noise is combined at different SNR (signal to noise ratio) with the impact acoustic signals experimentally obtained on the sample slabs to simulate the signals acquired under the actual inspection environments. Finally the classification results achieved with the present method are compared with that with the classic frequency-domain artificial neural network (ANN) classifier.

2. Wavelet transform and hidden Markov models

2.1. Basis of wavelet transform

Defined in terms of basis functions obtained by compression/dilation and shifting of a mother wavelet, the wavelet acts as a mathematical microscope which allows one to zoom in the fine structure of a signal, or alternatively, to reveal larger scale structures by zooming it out. In contrast to the Fourier transform, which lacks the time domain resolution, the wavelet transform is appropriate for the processing of time variant signals since it can give the information about the signals both in frequency and time domains.

The continuous wavelet transform (CWT) of $f(t)$ [20] is defined as:

$$CWT(a,b) = \int_{-\infty}^{+\infty} f(t)\psi_{a,b}(t)\,\mathrm{d}t, \tag{1}$$

where

$$\psi_{a,b}(t) = \frac{1}{\sqrt{|a|}}\psi\left(\frac{t-b}{a}\right) \quad a,b \in R; a \neq 0 \tag{2}$$

where $\psi_{a,b}(t)$ denotes the mother wavelet, a represents the wavelet scale index which is reciprocal of frequency and b indicates the time shifting.

The discrete wavelet transform DWT is derived from the discretization of CWT(a,b) given by

$$DWT(j,k) = \frac{1}{\sqrt{2^j}}\int_{-\infty}^{+\infty} f(t)\psi\left(\frac{t-2^j k}{2^j}\right)\mathrm{d}t, \tag{3}$$

where a and b are replaced by 2^j and $2^j k$. An efficient way to implement this scheme based on Mallat algorithm [26] using filters can be developed. In the decomposition step, the discrete signal is convolved with a low pass filter L and a high pass filter H, producing two output vectors cA1 and cD1. The elements of these vector cA1 are called Approximate Coefficients and the elements of the vector cD1 are called Detailed Coefficients respectively. The down sampling process, by which the odd indexed elements of the filtered signal are omitted, is carried out to ensure that the whole number of the coefficients produced by the basic decomposition step is approximately the same as the number of the elements of the original discrete signal.

2.2. Basis of hidden Markov models

As the HMM is well described in many literatures [23–25], its concept is only briefly reviewed in this section. An HMM is a finite state statistical structure with a fixed number of states, which is particularly well suited for the statistical characterization of nonstationary signals such as speech and time-varying noise. The underlying assumption of the HMM is that the time series signal can be well characterized as a parametric random process and that the parameters of the stochastic process can be estimated in a well defined manner. HMM is a doubly embedded stochastic process with an underlying stochastic process that is not directly observable, but can be observed only through another set of stochastic processes that produce the sequence of observations [23].

Usually, the HMM contains finite number of states, where each state generates an observation at a certain time point. The hidden state behavior is characterized by a transition probability matrix, an observation probability distribution, and an initial state probability distribution which has to be calculated from an HMM. In summary, the complete specification of an HMM includes the following elements:

(1) set of hidden states:

$$S = \{S_1, S_2, \ldots, S_N\}, \tag{4}$$

where N is the number of states in the model;

(2) state transition probability matrix

$$A = \{a_{ij}\} \tag{5}$$

where $a_{ij} = P[q_{t+1} = S_j | q_t = S_i]$, for $1 \le i,j \le N$, where q_t represents the hidden state at time t;

(3) set of observation symbols:

$$O = \{o_1, o_2, \ldots, o_M\} \tag{6}$$

where M is the number of possible observation symbols per state. The observation may be either discrete or continuous. In the present work, it is considered as continuous Gaussian observation.

(4) observation symbol probability distribution

$$B = \{b_j(O_t)\} \tag{7}$$

where $b_j(O_t) = N(M_j, \sum_j)$ for $1 \le i,j \le N$, where M_j is the observation mean vector in the state j and $\sum_j$ is the observation covariance matrix in state j.

(5) initial state probability distribution

$$\pi = \{\pi_i\}, \tag{8}$$

where $\pi_i = P[q_1 = S_i]$, for $1 \le i \le N$,

A hidden Markov model can be defined by the triplet $\lambda = \{A, B, \pi\}$ [23,25]. The observation may be either discrete or continuous. In the continuous case as this paper, it is considered as continuous Gaussian observation. Thus $\lambda = \{A, \pi, M, \sum\}$. In general, at each instant of time, the model is in one of the states $q_t = S_i$. It outputs observation O_t with probability $b_i(O_t)$ and then jumps to state $q_{t+1} = j$ with probability a_{ij}. The model may be obtained off-line by training. The state transition matrix represents the structure of the HMM.

The structure of the models defines the constraints on the elements in the state transition matrix A. The left-to-right models [23] are typically used to model temporal sequences in extensive applications like speech recognition, underwater acoustic target classification and electrocardiogram (ECG) signal recognition. An example of three-state HMM is shown in Fig. 1. They have the following properties: (1) The first observation is produced when the Markov chain is in the first state; (2) The last observation is generated when the Markov chain is in the final state; and (3) It is straightforward that the transition behavior of the left-to-right model, in which there is no possibility to go back to a precedent state, exhibits high consistence with the temporal pattern of time series associated with certain statistical model.

3. Experimental results

3.1. Experimental configuration

In order to investigate the practical characteristics of the impact-acoustics signature, experiments are carried out on some artificial sample slabs. To simulate the possible physical bonding conditions, 3 types of sample slabs are prepared as specified by the Hong Kong Housing Authority. One is a tiled-concrete slab of good bonding strength (referred to as "solid1" class). The second type of tiled-slab contains a $\varnothing$140 mm circle-shaped void at the center location in the concrete substrate layer (referred to as "void" class).

As the technique is only required to identify the bonding condition of the tiles, the two aforementioned types of slabs should be sufficient for the experiments in principle. However, it has been observed that the abnormal multiple contacting behaviors caused by the surface irregularity greatly affect the actual acoustic characteristics [15–18]. Also, in the actual site trials, quite a significant number of the wall surfaces are not smooth at all. So the third type of sample slabs is specially prepared to feature good bonding integrity but with rough surface near the edges of tiles (referred to as "solid2" class). The dimensions of all the slabs are: 400mm × 400mm × 150 mm.

The nondestructive testing (NDT) experimental system is illustrated in Fig. 2. The apparatus adopted includes: a rigid steel sphere of diameter 12 mm pushed by a coil used as the controlled impactor, a pre-amplifier module, an A/D converter

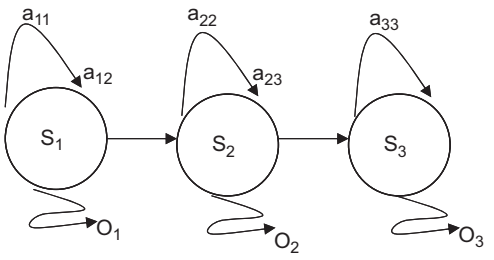

Fig. 1. Illustration of left–right HMM.

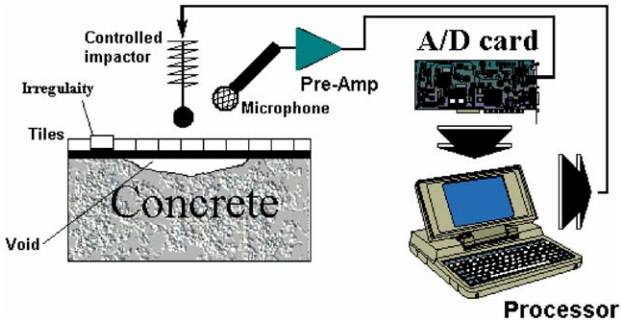

Fig. 2. The system block diagram of the impact acoustic inspection device.

card with 40 kHz sampling rate and a highly directional microphone. Such a setup provides a robust and cost-effective system for generating the required impact forces on the tile-walls and collecting the impact sounds for further signal processing and interpretation. The system is also compact and light enough to be carried by various climbing robots [3–5].

3.2. Signature obtained and analysis

3.2.1. Classic frequency domain analysis

In time-domain, each time history contains 512 signal points sampled at 40 kHz, triggered by the pulse used to activate the impactor. To obtain the frequency-domain information, the power spectral density (PSD) of the signature is obtained with the 512-point fast Fourier transform (FFT) calculation based on the original time history. To remove the influence of impact strength, the resulting PSD is then normalized with its maximal magnitude to get the normalized PSD.

The typical signals obtained experimentally are illustrated in Figs. 3–5. From the resulting PSD curve obtained from the "solid1" class slab as shown in Fig. 3(b), a ring peak located around 8–10 kHz is observed, which corresponding to the steel sphere's ringing as pointed out by [17,18]. Meanwhile the spectral components within 0–8 kHz obtained from the "void" class slab as shown in Fig. 5(b) are concluded to be associated with the multiple mode flexural vibration of the target structure. According to previous analysis [17,18], the high energy distribution of these two components may indicate the presence of bonding defects, which provides a theoretical basis for the classic spectral method.

However, for the "solid2" class slab which has good bonding integrity but with an irregular surface, a single tap on the rough surface can cause the impactor sphere to have multiple bounces on the target surface [15,17,18]. Due to the multiple bounces, the resulting time history contained multiple acceleration peaks and relatively weak ringing component (See Fig. 4(a)). As a result, the corresponding PSD curve as shown in Fig. 4(b) exhibits patterns similar to that of the debonded cases (See Fig. 5(b)) in the corresponding frequency ranges.

The above experimental analysis shows that, for the case of normal impact, the distribution of PSD curve can clearly indicate the existence of bonding defects and hence can be used as an indicator for characterizing bonding condition as reported by previous works [15–18]. However, a tap on an irregular surface will impose difficulty on identifying bonding condition due to the overlapping pattern in PSD caused by multiple bounces of the impactor head on the target surface.

To study and to develop a technique to overcome the effect of environmental noise, real noise recorded at a typical inspection site is combined with the corresponding impact sound to test the classification performance in noisy inspection environments. As the noise acquisition site is located next to a main road and a building under maintenance, the obtained environmental noise is the mixture of traffic noise, speech noise and mechanical noise, which are the typical noise in tile-wall inspection operation. The normalized PSD curves of the real environmental noise are shown as green dashed lines in Figs. 6(b), 7(b) and 8(b), which indicate that low frequency range contains most components of the real noise. Herein the *signal to noise ratio* (SNR) is defined as:

$$SNR = 10\log\left[\frac{\mathrm{var}(Signal)}{\mathrm{var}(Noise)}\right] \tag{9}$$

where var(x) denotes the variance of the 512 samples of sequence x. Under the SNR of 0 dB, the resulting noisy time histories, PSD curves as well as the DWT results for the three different classes of concrete slabs are provided in Figs. 6–8. As show in Figs. 6(b), 7(b) and 8(b), the PSD curves of the "solid1", "solid2" and "void" class exhibit more similarities due to the increasing PSD level in the lower frequency range caused by the mixture of the real noise. Furthermore, it can also be seen from the Figs. 6(a), 7(a) and 8(a) that the signal distortion caused by the noise will hinder the extraction of the initial acceleration pattern and pose tremendous difficulties to the method based on the initial acceleration behavior [17].

3.2.2. DWT analysis

For the aim of comparison, the "clean" and "noisy" signals from the three classes of concrete slabs are processed with the DWT. According to the Nyquist's rule, the maximum frequency of the impact signals is 20 kHz determined by the

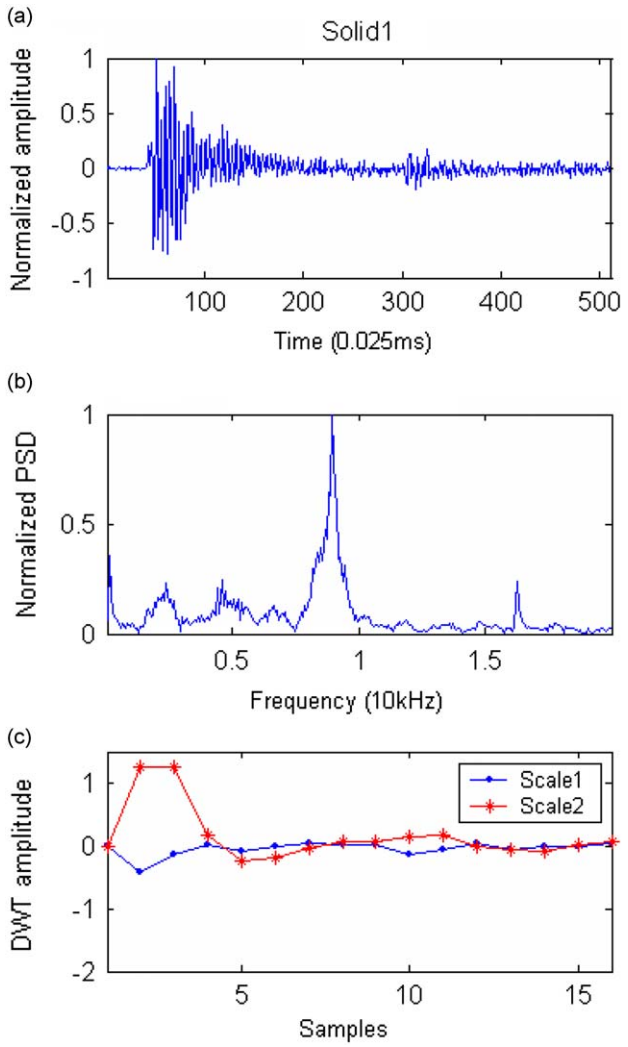

Fig. 3. Time history (a), PSD (b) and DWT coefficients (c) of typical impact sound from "solid1" class slab.

adopted sampling frequency of 40 kHz. The impact acoustic signals are then decomposed up to 5 levels using Daubechies1 (db1) mother wavelet. The frequency bandwidths of Approximation and Detail coefficients of wavelet decompositions are shown in Fig. 9. In the 5th level, the DWT scales where the impact sound signal reigns most are identified via the wavelet decomposition on the sample signals. The finally selected DWT scales, corresponding to the frequency band of 5.625–6.25 kHz (called Scale1) and 7.5–8.125 kHz (called Scale2) respectively as shown in grey blocks in Fig. 9, are considered to represent the main temporal information contained in the signal components from the impactor and the target structure; these two DWT scales are found to contain the dominant energy of the resonant components of the impactor and the debonded target structure.

Figs. 3(c), 4(c) and 5(c) show the DWT coefficients of the 2 selected scales of the "clean" impact sound signals obtained from three different classes of the slabs. It can be observed that, in the case of the "solid2" class which previously shows similar patterns in the PSD curve with the "void" class, the corresponding temporal coefficients of the two DWT scales generally exhibit time-frequency behaviors different from the void class. The main observations from Figs. 3(c), 4(c) and 5(c) can be summarized as follows:

(1) For the cases of "solid2" and "void" class, the DWT coefficients of the 2 selected scales exhibit a prolonged oscillation while those of "solid1" class settle to a steady value quickly. These prolonged oscillations can generally be interpreted to be caused by the multiple bounces in the "solid2" case and the nature of multiple-model flexural ringing associated with the "void" class.

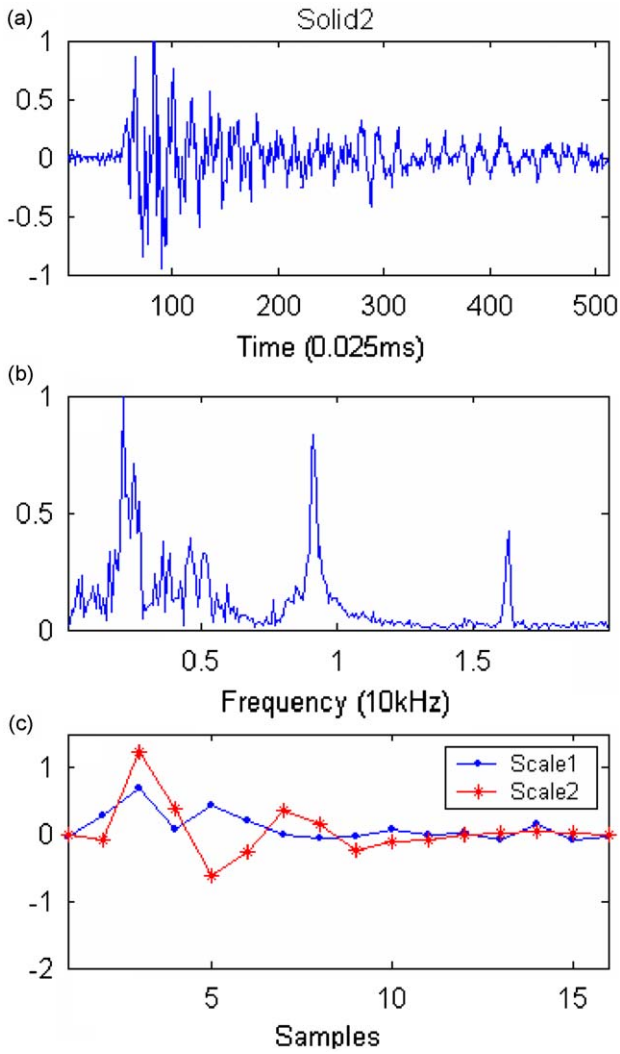

Fig. 4. Time history (a), PSD (b) and DWT coefficients (c) of typical impact sound from "solid2" class slab.

(2) Next, in the case of the "void" class, the DWT coefficients of Scale1 show a stronger peak than that of Scale2, whereas both "solid1" and "solid2" case, on the other hand, exhibit higher peaks at the DWT coefficients of Scale2 (See Figs. 3(c), 4(c) and 5(c)). This indicates that different bonding classes have different energy distribution.

(3) Regarding the relative arrival time of the strongest peak, those at both scales in the "solid1" and "solid2" cases arrive almost simultaneously. However, for the "void" case, the first peak of Scale1 comes generally earlier than that of Scale2, revealing the different temporal pattern with different bonding quality.

Thus, from the above signal analysis in the DWT domain, it can be concluded that the temporal pattern of the DWT coefficients in the 2 selected scales may provide an effective way to identify the different bonding qualities and surface roughness.

Figs. 6(c), 7(c) and 8(c) show the DWT decomposition of the three types of impact sounds contaminated by real noise. As seen in the plots, the temporal behaviors of the 2 DWT scales show high tolerance to the impairment of noise; the above three features found in the "clean" signals still exist in Figs. 6(c), 7(c) and 8(c). The reason is that the zoom ability of the DWT can focus in the scales where signal components dominate, thus suppresses the noise from the other scales. As a result, unlike the features adopted in classic spectral and time-domain method which are generally too sensitive to noise, features in DWT domain show relatively enhanced noise robustness.

From the results of signatures analysis, it is seen that the wavelet domain features would outperform the classic spectral feature based method in discriminating the impact sound from "solid2" and "void" slabs. Moreover, with the help of the wavelet decomposition, the features can be extracted from the selected DWT scales in which the signal component plays a dominant role to alleviate the impairment of the noise. In this paper, with the features extracted via DWT, a novel

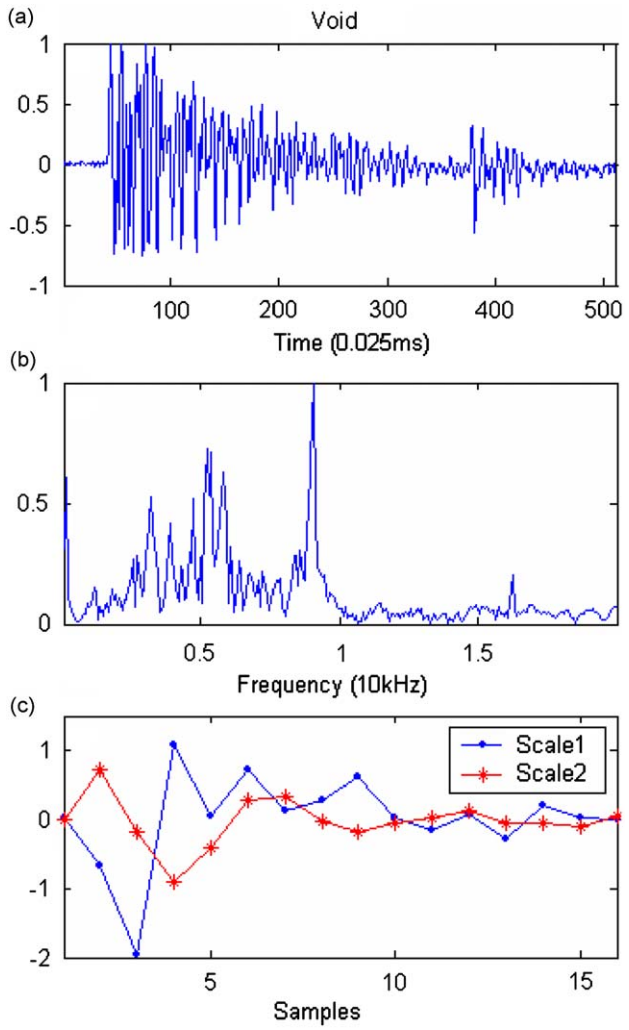

Fig. 5. Time history (a), PSD (b) and DWT coefficients (c) of typical impact sound from "void" class slab.

statistical model based inspection approach is proposed to facilitate a robust assessment of tile-wall bonding integrity at the presence of the surface irregularities and the environmental noise.

4. Fault recognition via the proposed method

4.1. Recognition via HMM

As mentioned above, unlike the classic "feature-based" recognition system, the HMM-based strategies try to achieve superior performance by uncovering the underlying system statistical model behind the external features. In this research work, HMM is employed as the model-based classifier to perform the inspection in order to facilitate the robust signal interpretation and classification. The time-frequency domain features with a dimension of 2-row and 16-column extracted from two selected DWT scales are adopted as the input of the HMM to characterize the statistical models associated with different bonding integrity and surface roughness. The HMM based recognition method generally consists of the training and classification process. Regarding the proposed tile-wall bonding integrity assessment system, "solid1", "solid2" and "void" class are firstly trained with HMM respectively through the training sets obtained from the corresponding artificial slabs.

The HMM training process is to estimate the model parameter set from the observation sequence **O**. The HMM parameter estimation is carried out by the Baum–Welch method (expectation-maximization method) [27]. According to different bonding integrity of "solid1", "solid2" and "void" class, each corresponding HMM is adapted to its respective time-frequency patterns using the DWT features of the training sets. To model the temporal behaviors in 2 selected DWT scales, 2-order state is applied. To achieve a good compromise on computational complexity versus performance, the

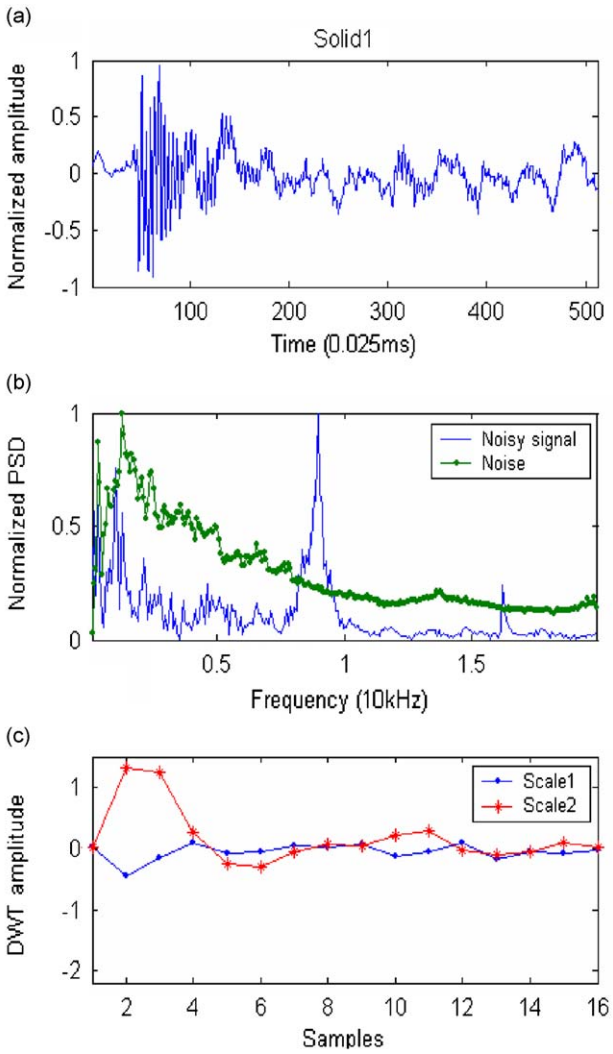

Fig. 6. Time history (a), PSD (b) and DWT coefficients (c) of typical impact sound from "solid1" class with noise.

number of the 2-order states of each model was specified empirically after some simulations. The length of the DWT domain observation sequence must be carefully chosen to reduce the computation time while at the same time retain enough information to capture the time-frequency features of the signal. In the present work, the DWT domain sequence length of 16 is adopted accordingly.

After the training procedure, the HMM models of different bonding states are tested with the test set. With the DWT features from each type of sample adopted as the input, the model likelihood of each model is calculated, among which the model associated with highest likelihood is considered as the best candidate representing the current bonding integrity, as shown in Fig. 10.

4.2. Classification results

In this study, impact sounds obtained in the laboratory with 3 typical sample specimens mentioned above are firstly divided into a training set and a "clean" test set. The training set is used to train the HMM and the trained HMM is then evaluated with the test set. The training set contains 200 samples of "solid1", 200 samples of "solid2" and 200 samples of "void" signatures. The test set contains the same number of samples. In the training process, the training set is randomly selected to provide enough information for the learning algorithm. In addition, two additional "noisy" test sets are obtained from the corresponding signals in "clean" test set by mixing the data with real noise at SNR of 3 and 0 dB in order to validity the performance under noise. The real background noise is the same as that used in the signal analysis section. For the aim of comparison, the training set, "clean" test set and "noisy" test set are also applied to a classic frequency-domain feature based ANN (artificial neural networks) classifier. To match the feature dimension used in the proposed

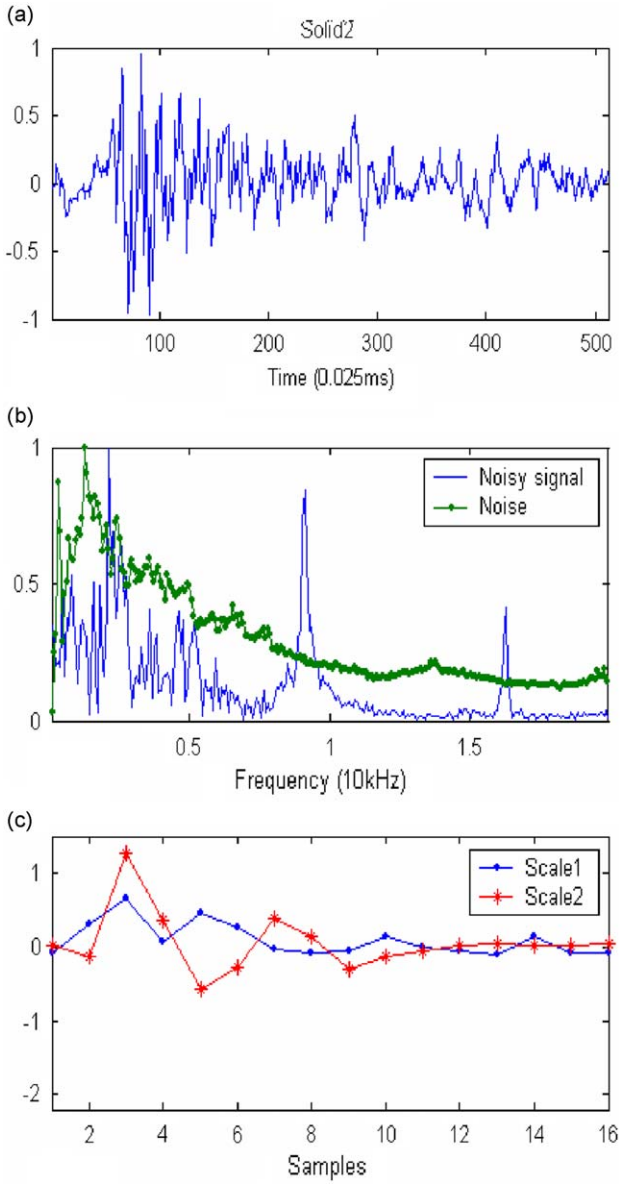

Fig. 7. Time history (a), PSD (b) and DWT coefficients (c) of typical impact sound from "solid2" class with noise.

approach, the whole PSD of the impact sounds was divided into 32 equal intervals, and the area of each was extracted as feature to be used as an input of the three-layer BP neural network classifier consisting of a 32-node input layer, 8-node hidden layer as well as a two-node output layer. The classification results obtained with the proposed DWT–HMM classifier and the PSD–ANN classifier are presented in Tables 1 and 2 respectively.

In this study, the effects of the surface roughness as well as the real environmental noise are considered. As shown in Table 1, under the "clean" environment where no noise is added, with the feature vectors extracted from the DWT as the input to the HMM, the accuracy rate is 99.5% for both "solid1" and "solid2" class and 100% for the debonded case. This indicates that the proposed approach has a good discriminating ability with respect to the bonding property and surface roughness. Utilizing the classic PSD–ANN classifier, the classification rate of the "solid1", "solid2" and "void" class is 93%, 90.5% and 97% respectively for the "clean" test set (See Table 2), indicating performance degradation caused by the surface irregularity.

For the noisy case, the accuracy rate obtained from the proposed HMM approach shows high immunity to noise as shown in Table 1. When the SNR of the additive background noise is 3 dB, the accuracy rate exhibits a tiny drop to 98%, 98.5% and 95.5% for the "solid1", "solid2" and "void" classes respectively. Even for the signals contaminated with 0 dB environmental noise, it can still achieve the accuracy rates of 93%, 91% and 92.5% for the "solid1", "solid2" and "void" class

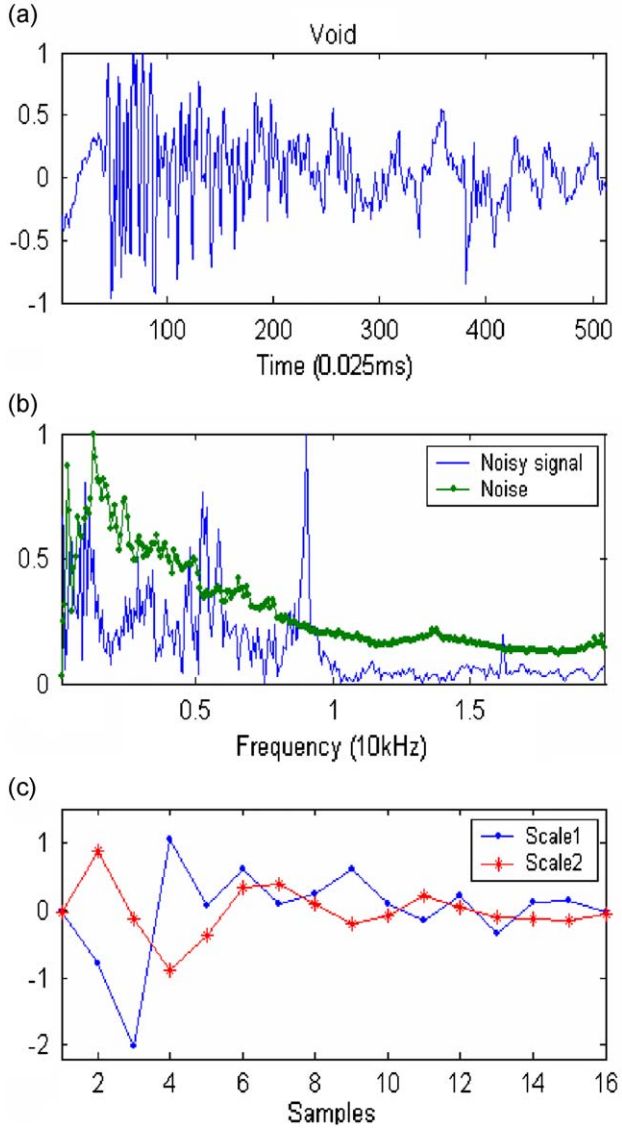

Fig. 8. Time history (a), PSD (b) and DWT coefficients (c) of typical impact sound from "void" class with noise.

respectively. On the other hand, the accuracy rate obtained from the PSD–ANN method for the "solid1", "solid2" and "void" class is 86.5%, 88% and 93% respectively when the noise has the SNR value of 3 dB, which further falling to 76%, 79.5% and 84.5% respectively when the SNR is 0 dB, as shown in Table 2.

5. Conclusions

In the present work, an NDT method based on acoustic features is investigated to improve the robustness in the tile-wall bonding integrity inspection. Most of the previous research employed the classification approaches based on the features extracted directly in the frequency domain and the classic feature-based classifier, which are found to be too sensitive to the feature mismatch caused by the multiple bounces on irregular surfaces as well as the environmental noise. As a result, the practical implementation of the impact testing method for tile-wall inspection has not been used widely since quite a significant number of the tile-wall finishes are not very smooth especially for the public housing estates. Besides, the working environments are usually noisy. In view of these problems, a novel NDT strategy based on the simultaneous adoption of the DWT domain features and the HMM based classifier has been developed to provide a quantitative automatic tile-wall inspection with better immunity to noise and surface irregularity.

Due to the nature of the Fourier transform, the features extracted from the PSD can only reveal the global frequency distribution pattern of the signal through the whole sampled length, while containing no information of the temporal

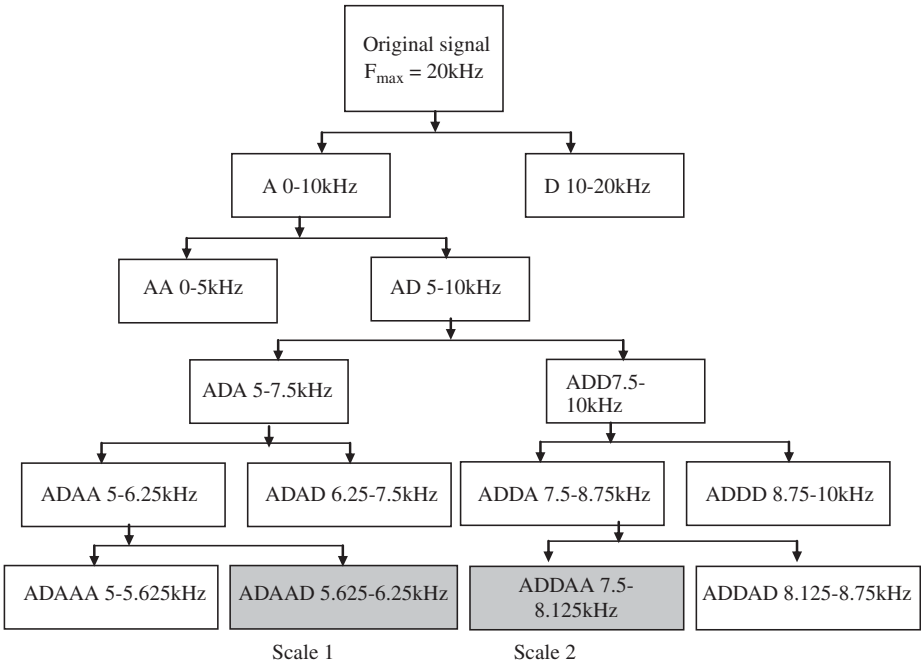

Fig. 9. Scales and the associated frequency band of the DWT.

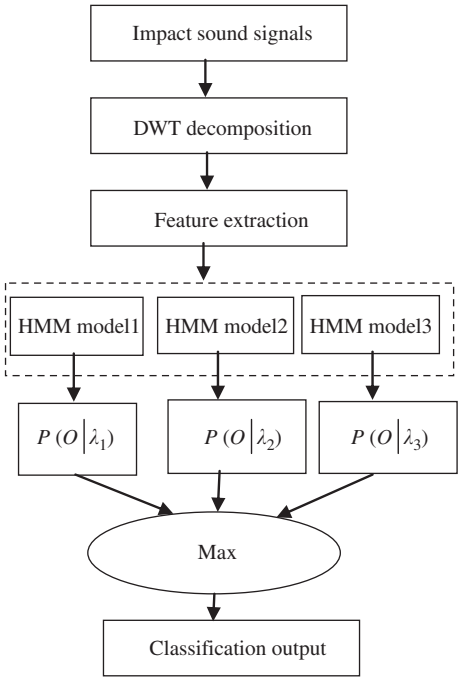

Fig. 10. Block chart of HMM classifier.

behavior. In contrast, this paper adopted the wavelet transform to offer a comprehensive way to extract the temporal as well as spectral pattern of the target signal. Moreover, an additional innovation of this paper is to utilize the internal mechanism behind the impact sounds by modeling the temporal characteristics of the impact signals at the selected DWT scales with the HMM.

Classification experiments carried out with the help of artificial slabs demonstrate that, while the existence of the surface non-uniformity as well as noise seriously deteriorate the performance of the classic PSD–ANN classifier, the proposed DWT–HMM strategy exhibits high tolerance to the problems of noise and multiple bounces. The classification

Table 1
Classification results with proposed DWT–HMM method.

	Type	Classification output			Accuracy rate (%)
		Solid1	Solid2	Void	
Without noise	solid1	198	2	0	99
	solid2	1	199	0	99.5
	void	0	0	200	100
SNR=3 dB	solid1	196	3	1	98
	solid2	3	197	0	98.5
	void	0	9	191	95.5
SNR=0 dB	solid1	186	12	2	93
	solid2	15	182	3	91
	void	0	15	185	92.5

Table 2
Classification results of PSD–ANN(power spectrum density–artificial neural networks) classifier.

	Type	Classification output			Accuracy rate (%)
		Solid1	Solid2	Void	
Without noise	solid1	187	13	0	93.5
	solid2	7	181	4	90.5
	void	0	6	194	97
SNR=3 dB	solid1	173	24	3	86.5
	solid2	17	176	7	88
	void	0	14	186	93
SNR=0 dB	solid1	152	45	3	76
	solid2	26	159	14	79.5
	void	0	31	169	84.5

performance based on signatures of different bonding quality, surface roughness and SNR is presented and compared. The results have demonstrated the effectiveness of the presented method in alleviating the impairment of abnormal impacts and noise. In view of the enhanced tolerance to external interferences, the proposed NDT method has a high potential to be developed into a low-cost, reliable and convenient NDT system for automatic inspection of tile-wall bonding integrity under harsh operation environments.

Acknowledgment

The authors are grateful for the funding by a grant from City University of Hong Kong (Project no. 9610024-630: ITRG006-06) in support of the present research.

Appendix A. Supplementary material

Supplementary data associated with this article can be found in the online version at doi:10.1016/j.jsv.2009.11.038.

References

[1] M.Y.L. Chew, Factors affecting ceramic tile adhesion for external cladding, *Construction and Building Materials* 13 (1999) 293–296.
[2] K.S. Tan, K.C. Chan, B.S. Wong, L.W. Guan, Ultrasonic evaluation of cement adhesion in wall tiles, *Concrete Composites* 18 (1996) 119–124.
[3] B.L. Luk, D.S. Cooke, S. Galt, A.A. Collie, S. Chen, Intelligent legged climbing service robot for remote maintenance applications in hazardous environments, *Journal of Robotics and Autonomous Systems* 53/2 (2005) 142–152.
[4] B.L. Luk, A.A. Collie, D.S. Cooke, S. Chen, Walking and climbing service robots for safety inspection of nuclear reactor pressure vessels, *Journal of Measurement and Control* 39/2 (2006) 43–47.
[5] B.L. Luk, K.P. Liu, A.A. Collie, D.S. Cooke, S. Chen, Tele-operated climbing and mobile service robots for remote inspection and maintenance in nuclear industry, *International Journal of Industrial Robot* 33/3 (2006) 194–204.
[6] S. Yang, L. Gu, R.F. Gibson, Nondestructive of weak joints in adhesively bonded composite structures, *Composite Structures* 51 (2001) 63–71.
[7] M. Sansalone, N.J. Carino, Detecting delaminations in concrete slabs with and without overlays using the impact-echo model, *Materials Journal of the American Concrete* 86 (1989) 177–184.

[8] M. Sansalone, W.B. Streett, *Impact-Echo NDE of Concrete and Masonry*, Bullbrier Press, Ithaca, N.Y., 2003.
[9] K. Mori, A. Spagnoli, A new non-contacting non-destructive testing method for defect detection in concrete, *NDT&E International* 35 (2002) 399–406.
[10] Y.H. Huang, S.P. Ng, L. Liu, C.L. Li, Y.S. Chen, Y.Y. Hung, NDT&E using shearography with impulsive thermal stressing and clustering phase extraction, *Optics and Lasers in Engineering* 47 (2009) 774–781.
[11] Y.Y. Hung, et al., Review and comparison of shearography and active thermography for nondestructive evaluation, *Materials Science and Engineering R* 64 (2009) 73–112.
[12] C. Meola, et al., Application of infared thermography and geophysical methods for defect detection in architectural structures, *Engineering Failure Analysis* 12 (2005) 875–892.
[13] T. Ito, T. Uomoto, Nondestructive testing method of concrete using impact acoustics, *NDT&E International* 30 (1997) 217–222.
[14] M. Asano, T. Kamada, M. Kunieda, K. Rokugo, Impact acoustics methods for defect evaluation in concrete, *Proceedings of Nondestructive testing-Civil Engineering 2003* (*NDT-CE2003*), 〈http://www.ndt.net/article/ndtce03/papers/v040/v040.htm〉.
[15] H. Wu, M. Siegel, Correlation of accelerometer and microphone data in the "Coin Tap Test", *Proceedings of the Instrumentation and Measurement Technology Conference99*', vol. 2, May 24–26, 1999, pp. 814–819.
[16] F. Tong, X.M. Xu, B.L. Luk, K.P. Liu, Evaluation of tile-wall bonding integrity based on impact acoustics and support vector machine, *Sensors and Actuators A: Physical* 144 (2008) 97–104.
[17] F. Tong, S.K. Tso, X.M. Xu, Tile-wall bonding integrity inspection based on time-domain features of impact acoustics, *Sensors and Actuators A: Physical* 132 (2006) 557–566.
[18] F. Tong, S.K. Tso, M.Y.Y. Hung, Impact-acoustics-based health monitoring of tile-wall bonding integrity using principal component analysis, *Journal of Sound and Vibration* 294 (2006) 329–340.
[19] S.P. Song, P.W. Que, Wavelet based noise suppression technique and its application to ultrasonic flaw detection, *Ultrasonics* 44 (2006) 188–193.
[20] V. Purushotham, S. Narayanan, S.A.N. Prasad, Multi-fault diagnosis of rolling bearing elements using wavelet analysis and hidden Markov model based fault recognition, *NDT&E International* 38 (2005) 654–664.
[21] M. Ge, R. Du, Y. Xu, Hidden Markov model based fault diagnosis for stamping processes, *Mechanical Systems and Signal Processing* 18 (2004) 391–408.
[22] J.M. Lee, S.J. Kim, Y. Hwang, C.S. Song, Diagnosis of mechanical fault signals using continuous hidden Markov model, *Journal of Sound and Vibration* 276 (2004) 1065–1080.
[23] A.-A. Tarik, Y. Hamam, R. Fodil, F. Lofoso, D. Isaley, Using hidden Markov models for sleep disordered breathing identification, *Simulation Modeling Practice and Theory* 12 (2004) 117–128.
[24] T.L. New, S.W. Foo, L.C. De Silva, Speech emotion recognition using hidden Markov models, *Speech Communication* 41 (2003) 603–623.
[25] Q. Miao, V. Makis, Condition monitoring and classification of rotating machinery using wavelets and hidden Markov models, *Mechanical Systems and Signal Processing* 21/2 (2007) 840–855.
[26] S.G. Mallat, A theory for multiresolution signal decomposition: the wavelet representation, *IEEE Trans Pattern and Machine Intelligence* 11 (1989) 674–693.
[27] X.D. Huang, Y. Ariki, M.A. Jack, *Hidden Markov Models for Speech Recognition*, Edinburgh University Press, 1990.